Chemosphere 291 (2022) 132828

Contents lists available at ScienceDirect

Chemosphere

journal homepage: www.elsevier.com/locate/chemosphere

Rice straw particles covered with *Brevundimonas naejangsanensis* DD1 cells can synergistically remove doxycycline from water using adsorption and biotransformation

Ting He [a,b,c], Jianguo Bao [a,**], Yifei Leng [d], Shuqiong Kong [a], Jiangkun Du [a], Xu Li [b,*]

[a] School of Environment Studies, China University of Geosciences, Wuhan, 430074, PR China
[b] Department of Civil and Environmental Engineering, University of Nebraska-Lincoln, Lincoln, NE, 68588, USA
[c] Institute of Chemistry, Henan Academy of Sciences, Zheng Zhou, Henan Province, 450002, PR China
[d] School of Civil Engineering, Architecture and Environmental, Hubei University of Technology, Wuhan, 430068, PR China

HIGHLIGHTS

- Rice straw particles (RSPs) were covered with a doxycycline degrading bacterium DD1.
- DD1-covered RSPs had faster DC removal kinetics than DD1 biotransformation alone.
- DD1-covered RSPs had higher DC removal efficiencies than RSP adsorption alone.
- New DC biotransformation products were identified.

GRAPHICAL ABSTRACT

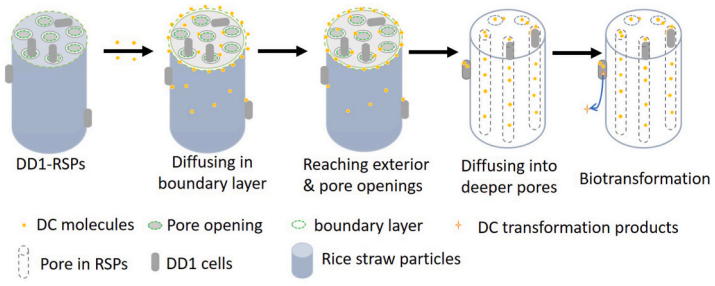

ARTICLE INFO

Handling Editor: Y Yeomin Yoon

Keywords:
Doxycycline
Adsorption
Biotransformation
Rice straw particles

ABSTRACT

Doxycycline (DC) is a second generation tetracycline antibiotic and its occurrence in the aquatic environment due to the discharge of municipal and agricultural wastes has called for technologies to effectively remove DC from water. The objective of the study was to characterize the synergistic benefits of adsorption and biotransformation in removing DC from water using rice straw particles (RSPs) covered with DC degrading bacteria, *Brevundimonas naejangsanensis* strain DD1. First, optimal experimental conditions were identified for individual processes, i.e., hydrolysis, adsorption, and biotransformation, in terms of their performance of removing DC from water. Then, synergistic effects between adsorption and biotransformation were demonstrated by adding DD1-covered RSPs (DD1-RSPs) to DC-containing solution. Results suggest that DC was quickly adsorbed onto RSPs and the adsorbed DC was subsequently biotransformed by the DD1 cells on RSPs. The adsorption of DC to DD1-RSPs can be well described using the pseudo-second-order kinetics and the Langmuir isotherm. The DD1 cells on RSPs converted DC to several biotransformation products through a series of demethylation, dehydration, decarbonylation, and deamination. This study demonstrated that adsorption and biotransformation could work synergistically to remove DC from water.

* Corresponding author. 900 N 16th St., W150D, Nebraska Hall, Lincoln, NE, 68588-0531, USA.
** Corresponding author. No. 388 Lumo Road, Wuhan, Henan Province, 430074, PR China.
E-mail addresses: bjianguo@cug.edu.cn (J. Bao), xuli@unl.edu (X. Li).

https://doi.org/10.1016/j.chemosphere.2021.132828
Received 22 August 2021; Received in revised form 3 November 2021; Accepted 6 November 2021
Available online 8 November 2021

1. Introduction

Tetracyclines (TCs) are a class of widely used antibiotics (Liu et al., 2019). Compared to the first-generation TCs, doxycycline (DC) has higher lipophilicity (Spina-Cruz et al., 2019), higher bioavailability, shorter half-life, and stronger antibacterial potency (Yan et al., 2018). Hence, DC has gradually become a safer alternative to other TCs (Heaton et al., 2007), and has been frequently used on livestock (Widyasari-i-Mehta et al., 2016) and aquaculture (Yan et al., 2018), as well as in human therapy (2018). Because the DC ingested can be released from excrement in its original form (Xu et al., 2021), DC has been detected in various environments, such as rivers (18–82 ng L^{-1}) (Deng et al., 2016), groundwater (0–39 ng L^{-1}) (Ma et al., 2015), wastewater (64–915 ng L^{-1}) (Lindberg et al., 2005), sludge (1.3–1.5 mg kg^{-1}) (Lindberg et al., 2005), sediments (0.23–0.32 μg kg^{-1}) (Fuentes et al., 2019), and soils (63–728 μg kg^{-1}) (Ho et al., 2014). Residual DC can cause teratogenic effects on aquatic organisms and promote the proliferation of resistance gene among microbes (Fan et al., 2019; Shao and Wu, 2020). Therefore, there is a need to develop treatment technologies to remove DC from water.

Abiotic processes, such as hydrolysis (Zaranyika et al., 2015), photocatalysis (Adamek et al., 2016; Bolobajev et al., 2016; Liu et al., 2018; Tong et al., 2019; Wang et al., 2019), advanced oxidation (Bolobajev et al., 2016; Zhang et al., 2016a; Spina-Cruz et al., 2019), and adsorption (Chao et al., 2014; Brigante and Avena, 2016; Zhang et al., 2016a, 2016b; Liu et al., 2017, 2019; Abbas et al., 2018; Bai et al., 2018; Zeng et al., 2018a, 2018b; Fan et al., 2019; Olusegun and Mohallem, 2019; Wei et al., 2019), have been reported effective in removing DC from water. Some novel adsorbents have been tested for their effectiveness in adsorbing DC. For example, graphene-like layered molybdenum disulfide can remove 90% of DC from solution in 8 h (Chao et al., 2014), and Cu(II) impregnated biochar can adsorb 93% of DC from water within 24 h (Liu et al., 2017). It is worth noting that while the adsorption process is simple and effective and can simultaneously remove multiple contaminants (Ahmed, 2016), it does not degrade DC (Gopal et al., 2020).

Biotransformation of antibiotic compounds have been reported. Tetracycline can be biotransformed by mixed community (Liao et al., 2021) and by pure culture (Leng et al., 2016). Biotransformation products of TC had lower antimicrobial potency than the parent compound and the transformation products from abiotic processes (He et al., 2021). So far, only a few papers reported the biotransformation of DC (Wen et al., 2018; He et al., 2021). Compared to some abiotic processes, DC biotransformation is a slower process and can be substantially affected by environmental factors (e.g., carbon source, temperature, and pH) (He et al., 2021).

Treatment processes that couple adsorption and biotransformation have the potential to synergistically remove contaminants from water. Such treatment processes have been successfully employed for water treatment and environmental remediation. One good example is the use of biologically active carbon to synergistically adsorb and biodegrade contaminants from water. In addition to adsorption, the adsorbent also provides a solid surface for biofilm growth (Xue et al., 2019), resulting in longer cell retention times, better protection of cells against environmental stress (e.g., pH and toxic compounds) (Lin et al., 2015), and higher tolerance to inhibitors (Ruan et al., 2018). Microbes immobilized on solid surface can biotransform the organic pollutants in water, such as phenol (Zhang et al., 2019), sulfamethoxazole (Xie et al., 2020), and TCs (Wu et al., 2020).

Some agricultural wastes are natural adsorbents (Dzionek et al., 2016) for DC, such as rice husk (80% removal in 24 h) (Zeng et al., 2018a), rice straw (88% in 24 h) (Zeng et al., 2018b), corn stalk (95% in 100 min) (Fan et al., 2019), and peanut shells (93% in 24 h) (Liu et al., 2017). Among them, rice straw has a loose, porous structure and contains reactive groups such as carboxyl and hydroxyl groups (Dai et al., 2018). The global production of rice straw is 600–900 million tons every year with most of it being burned in the field (Karimi et al., 2006). Hence, rice straw can be used as an abundant and environmentally friendly adsorbent for DC removal.

The objective of the study was to characterize the synergistic benefits of adsorption and biotransformation in removing DC from water using rice straw particles (RSPs) covered with DC degrading bacteria. RSPs and *Brevundimonas naejangsanensis* DD1, one of the first DC-biodegrading bacterial strains isolated from the environment, were used to make the bacteria-covered adsorbent, which was termed DD1-RSPs in this study. Environmental conditions were optimized for DC removal by DD1-RSPs (i.e., pH, background nutrient condition, and initial DC concentrations). The synergistic effects of biotransformation and adsorption in removing DC was characterized. The adsorption mechanism of DC by RSPs was also investigated. Furthermore, the biotransformation products of DC were identified and the biotransformation pathways were established. Finally, a conceptual model for the fate of DC on and in DD1-RSPs was proposed. The findings from this study demonstrate that DD1 covered RSPs can be an effective means to remove DC from water.

2. Materials and methods

2.1. Reagents, culture medium, and microorganism

All reagents were purchased from Aladdin (Shanghai, China), including analytical grade DC hydrochloride (MW = 480.90, $C_{22}H_{24}N_2O_8$·HCl, ≥99%), high performance liquid chromatography (HPLC) grade methanol and acetonitrile. Rice straw was collected from a paddy field in Jianghan Plain, Wuhan, Hubei. It was pulverized using a straw pulverizer, filtered through 60 mesh sieves (aperture <0.25 mm), washed 3 times using ultrapure water (Chen et al., 2017), and air dried. The resulting RSPs were sterilized using autoclave. Lysogeny broth (LB) medium contained 10 g L^{-1} tryptone, 5 g L^{-1} yeast extract, and 5 g L^{-1} NaCl. Mineral medium (MM) solution contained 1.5 g L^{-1} K_2HPO_4, 1.0 g L^{-1} NaCl, 0.5 g L^{-1} KH_2PO_4 and 0.2 g L^{-1} $MgSO_4$•$7H_2O$ (pH = 7.0) (Leng et al., 2016). MM-D solution was prepared by amending MM solution with 50 mg L^{-1} DC. MM-T solution was prepared by supplementing MM with 10 g L^{-1} tryptone, and MM-TD by amending MM-T with 50 mg L^{-1} DC. *Brevundimonas naejangsanensis* DD1 was isolated in a previous study (He et al., 2021). The 16S rRNA gene sequence of strain DD1 is deposited at GenBank under the accession number MT809477 (He et al., 2021).

2.2. Preparation of DD1- RSPs

To prepare the biologically active adsorbent, 1 mL (OD_{600} = 1) *B. naejangsanensis* DD1 was added to a 100-mL Erlenmeyer flask containing 50 mL LB medium and 0.3 g sterilized RSPs. The mixture was incubated on a shaker set at 150 rpm at 30 °C for 24 h to establish bacterial attachment on the surface of RSPs. The DD1-covered RSPs (DD1-RSPs) were washed three times using 0.85% NaCl solution and stored at 4 °C until use.

2.3. Investigation of DC removal by individual processes

Batch reactors were assigned to three groups: control group (50 mL MM-TD medium), adsorption group (50 mL MM-TD medium containing 0.3 g RSPs), and adsorption-biotransformation group (50 mL MM-TD medium containing 0.3 g DD1-RSPs). Based on the results of preliminary experiments, initial pH (i.e., 6, 7, 8, 9, 10), initial tryptone concentration (i.e., 2, 4, 6, 8, 10 g L^{-1}), and initial DC concentration (i.e., 50, 100, 150, 200 mg L^{-1}) were tested in separate experiments. All experiments were conducted for 72 h in dark at 20 °C on a shaker set at 150 rpm. The reactor solution was sampled at 0, 12, 24, 36, 48, 60, 72 h for analysis of residual DC concentrations. For all batch reactor tests, (1) the initial DC concentration was 50 mg L^{-1} unless stated otherwise; (2) MM-TD medium and RSPs were sterilized; (3) all experiments were

conducted under a biosafety cabinet; and (4) each experimental condition was tested with triplicate reactors.

2.4. Investigation of DC removal by DD1-RSPs

0.3 g DD1-RSPs were transferred to 100-mL Erlenmeyer flask containing 50 mL MM-TD medium at optimal conditions (pH = 7, tryptone = 4 g L^{-1}, DC = 50 mg L^{-1}) based on the results from Section 2.3. The mixture was incubated at 20 °C on a 150 rpm shaker in dark for 72 h. In addition to the reactors containing DD1-RSPs (i.e., hydrolysis + adsorption + biotransformation), three other groups of reactors were also included as controls: (1) reactors containing MM-TD solution only (hydrolysis group), (2) reactors containing MM-TD solution with 0.3 g RSPs (adsorption group), and (3) reactors containing MM-TD solution with 0.5 mL DD1 cells at OD_{600} = 1 (biotransformation group), respectively. The MM-TD medium and RSPs were sterilized, and all processes were operated in a biosafety cabinet. Liquid samples were collected from the reactors at 0, 0.5, 5, 10, 20, 30 min and 1, 2, 3, 4, 5, 6, 12, 24, 48, 72 h.

2.5. Distribution of DC on and in DD1-RSPs

0.3 g DD1-RSPs was transferred to 100-mL Erlenmeyer flasks containing 50 mL MM-TD medium. The operating conditions were the same as those described in Section 2.4. Samples were collected at 0.017 h (1 min), 0.17 h (10 min), 0.5 h (30 min), 1 h, 6 h, 24 h, 48 h, and 72 h to quantify DC in various portions of the solution. The methods for recovering DC from various portions of the solution were adopted from the literature (Song et al., 2016) and presented in Fig. 1. In brief, 3 mL of well-mixed mixture was collected and stood for 20 min to allow DD1-RSPs to settle. The suspension and the DD1-RSPs were further processed to separate the DC molecules associated with different compartments of the mixture. This test was conducted in triplicate reactors.

2.6. Modeling of adsorption

Equations for the isotherm and the kinetics of DC adsorption to RSPs are summarized in Table 1. The adsorption capacity was calculated via Equation (1). Pseudo-first-order and pseudo-second-order models were both tested to explain the kinetics of DC adsorption to RSPs. In addition, the rate control steps and the mechanism of DC adsorbed on RSPs were studied using the intra-particle diffusion model (Liu et al., 2017). The adsorption isotherms were simulated using models such as Langmuir, Freundlich and Temkin (Liu et al., 2017). Langmuir model assumes single-layer surface adsorption and no interactions between adsorbed molecules. Freundlich model is often used to analyze the adsorption process on heterogeneous surfaces. Temkin model considers interactions between adsorbed solutes.

Table 1
Kinetics and equilibrium isotherm equations.

No.	Mechanism	Equation
1	DC adsorbed on RSPs	$q_e = V(C_0 - C_e)/m$ (Chao et al., 2014) q_e: concentration of adsorbed DC at equilibrium (mg g^{-1}) C_0: initial DC concentration in medium (mg L^{-1}) C_e: residual DC concentration in medium at equilibrium (mg L^{-1}) V: the medium volume (L) m: the mass of rice straw particles (g)
2	Pseudo-first-order (Chao et al., 2014)	$\ln(q_e - q_t) = \ln q_e - k_1 t$ q_t: concentrations of adsorbed DC at time t (mg g^{-1}). k_1: DC adsorption rate constant of pseudo-first-order kinetics (h^{-1}) t: time
3	Pseudo-second-order (Chao et al., 2014)	$\frac{t}{q_t} = \frac{1}{k_2 {q_e}^2} + \frac{t}{q_e}$ k_2: DC adsorption rate constants of pseudo-second-order kinetics (g mg^{-1} h^{-1})
4	Intraparticle diffusion (Liu et al., 2017;Zeng et al., 2018b)	$q_t = k_p t^{0.5} + C$ k_p: the constant of intra-particle diffusion rate (mg g^{-1} $h^{1/2}$) C: intercept related to the thickness of the boundary layer (mg g^{-1})
5	Langmuir (Liu et al., 2017;Zaidi et al., 2019)	$q_e = \frac{K_L q_m C_e}{1 + K_L C_e}$ q_m: the maximum monolayer adsorption capacity of adsorbent for DC (mg g^{-1}) K_L: the Langmuir constant related to the energy of adsorption. (L mg^{-1})
6	Freundlich (Liu et al., 2017;Olusegun and Mohallem, 2019)	$q_e = K_f C_e^n$ K_f: the Freundlich constant representing the relative adsorption capacity of adsorbent ((mg g^{-1}) (mg L^{-1}) $^{-n}$) n: the exponential parameter indicative of adsorption intensity or surface heterogeneity (dimensionless)
7	Temkin (Dada et al., 2012)	$q_e = B \ln A_T + B \ln C_e$ A_T: Temkin isotherm equilibrium binding constant (L g^{-1}) B: constant related to the heat of adsorption (J mol^{-1})

2.7. Measurement of DC and identification of DC transformation products

Liquid samples were centrifuged at 8000 g for 10 min, then filtered through 0.22 μm filter and stored at −20 °C prior to DC measurements. Detailed quantification procedure can be found in our earlier paper (He et al., 2021). To identify transformation products, all samples were purified and concentrated using the Oasisa HLB (6 cc/150 mg, Waters) solid phase extraction column. All transformation products were identified using liquid chromatography mass spectrometry (Q Exactive system, Thermo scientific, USA). Finally, the Xcalibur 2.1 software (Thermo

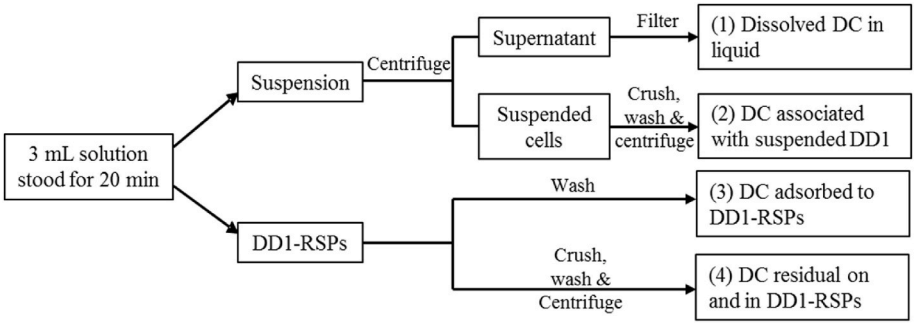

Fig. 1. The experimental procedure to separate the DC in the solution containing DD1-RSPs into portions associated with different compartments of the solution.

Scientific) was used for mass spectra analysis. The transformation products of DC were proposed based on the primary and secondary mass spectra: predicted mass (*m/z*), measured mass (*m/z*), error between predicted vs measured masses (<5 ppm), elemental composition, and intensity.

3. Results

3.1. The SEMs of DD1-RSPs

Fig. 2 showed the SEM images of the *B. naejangsanensis* DD1 cells, RSPs, and DD1-RSPs. DD1 cells had a rod shape and a length about 1 μm (Fig. 2A). RSPs exhibited porous structures where bacteria could occupy (Fig. 2B). For DD1-RSPs, DD1 cells are attached to the surface and pores of RSPs (Fig. 2C).

3.2. Individual transformation processes

The impacts of environmental factors (i.e., pH, initial tryptone concentration, and initial DC concentration) on individual processes involved in DD1-RSPs (i.e., hydrolysis, adsorption, and biotransformation) were tested. The raw DC concentration data from reactors containing RSPs and DD1-RSPs are reported in Fig. S1. Data processed to reflect the residual DC concentrations from individual processes are reported in Fig. 3. First, within the pH range tested (pH 6 to 10), hydrolysis and adsorption increased with pH (Fig. 3A–i and 3A-ii), while biotransformation decreased with increasing pH (Fig. 3A–iii). Second, the adsorption of DC on RSPs decreased with the increasing tryptone concentrations (Fig. 3B–ii). In contrast, hydrolysis and biotransformation of DC increased with increasing tryptone concentration (Fig. 3B–i and 3B-iii). Third, within the range of the initial DC concentrations tested (i.e., 50–200 mg L^{-1}), the adsorption reached equilibrium quickly (Fig. 3C–ii), while it took longer for the biotransformation to reach equilibrium (Fig. 3C–iii). DC residual concentrations normalized to initial concentrations reveal similar trends for the three mechanisms (Fig. S2). Finally, based on the results presented in Figs. 3 and S1, pH 7 and initial tryptone concentration of 4 g L^{-1} were chosen for future experiments.

3.3. Synergistic removal of DC by DD1-RSPs

DD1-RSPs achieved superior DC removal performance over RSPs or DD1 alone, in terms of both total removal and removal kinetics (Fig. 4). With hydrolysis alone, only 8.94% (4.5 mg L^{-1}) of DC was removed by the end of the 72-hr experiment. When biotransformation was the only mechanism, DD1 gradually reduced DC concentration from 50.0 mg L^{-1} to 13.9 mg L^{-1} over the course of 72 h. When adsorption was the only mechanism, DC concentration in solution was reduced from 50.0 mg L^{-1} to 12.8 mg L^{-1} within the first 4 h of the experiment but could not be further reduced in the remainder of the experiment. In comparison, when DD1-RSPs were used, DC removal followed a trend that combined the removal patterns from both adsorption and biotransformation. In the presence of DD1-RSPs, DC quickly dropped from 50.0 mg L^{-1} to 7.5 mg L^{-1} within the first 6 h, and continued to decrease to 1.5 mg L^{-1} by the end of the 72-hr experiment.

3.4. Distribution of DC

The temporal change of DC in each compartment of the solution mixture containing DD1-RSPs was characterized (Fig. 5). Prior to the addition of DD1-RSPs, all of the DC was in the liquid phase. At the beginning of the experiment (0.017 h, or 1 min), about half of the DC became associated with the DD1-RSPs matrix. Within the DC associated with the DD1-RSP matrix, some was adsorbed and could be washed off from DD1-RSPs while the rest was more tightly associated and cannot be washed off from DD1-RSPs. The DC dissolved in liquid and the DC associated with suspected cells decreased over time (Fig. 5). The DC adsorbed to DD1-RSPs remained nearly constant in the first hour of the experiment and started to decrease after that. The residual DC on and in DD1-RSPs slightly increased slightly first and then reduced later.

3.5. Adsorption mechanism of DC by RSPs

The adsorption of DC by RSPs reached equilibrium in the first 6 h (Fig. 6A). Compared to the pseudo-first order kinetics, the pseudo-second order kinetic model can better describe the adsorption kinetics of DC to RSPs (Table S1, R^2 = 0.9764). Besides, the intra-particle diffusion model shows that there were three phases during the DC adsorption onto RSPs (Fig. 6B and Table S2). The diffusion rate constants for the three phases are 2.2868, 1.3890, and 0.2338, respectively (Table S2). The adsorption process gradually slowed down and stabilized. Finally, compared to the other two isotherm models tested (Fig. 6C), the Langmuir model fitted the experimental data the best with R^2 of 0.9933 (Table S3).

3.6. Transformation products

Transformation products of DC were identified (Table 2) and were used to establish transformation pathways (Fig. 7). Three transformation products were detected in reactors containing RSPs: DP-461, DP-459, and DP-443. Nine transformation products were formed in the presence of DD1-RSPs: DP-461, DP-443, DP-428, DP-417, DP-410, DP-402, DP-400, DP-338, DP-323. The isomer (Iso-DC) and epimer (EDC) of DC were the only transformation products found in reactors containing no RSPs or DD1-RSPs, suggesting they were the hydrolysis products of DC.

DC was biotransformed through three potential pathways. In the first pathway, which was reported in our previous study (He et al., 2021), DC was biotransformed to DP-417, DP-402, DP-338, to DP-323 (i.e., the pathway shown in the top portion of Fig. 7). In the second pathway, DC

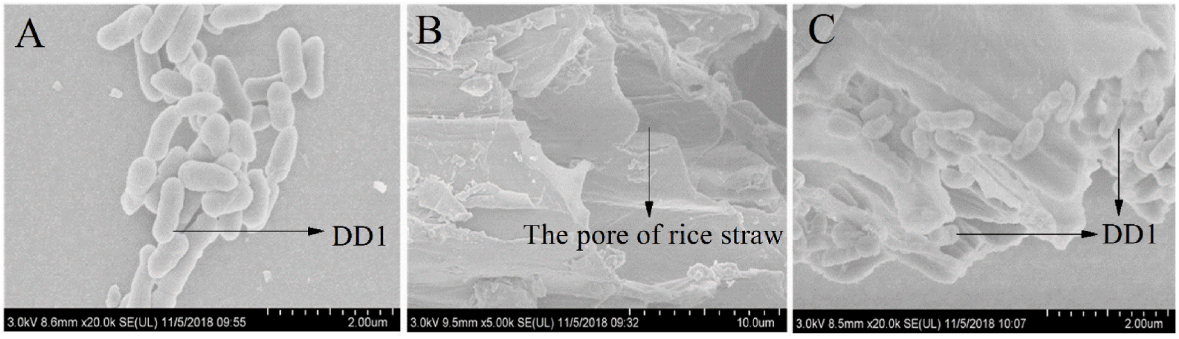

Fig. 2. SEM images of the pure culture of *B. naejangsanensis* strain DD1 (A), RSPs (B), and DD1-RSPs (C).

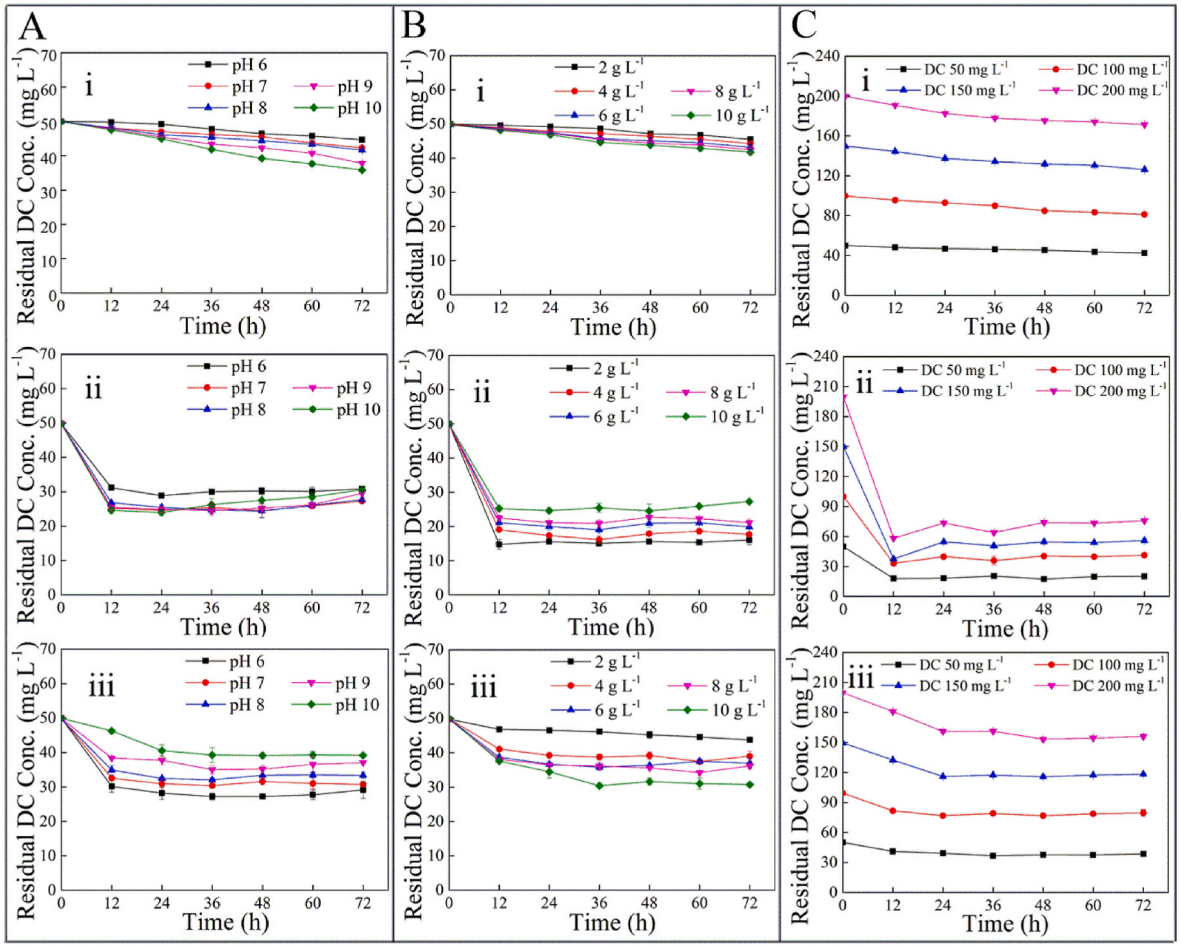

Fig. 3. The change of DC concentrations due to hydrolysis only (i), absorption only (ii), and biotransformation only (iii) at different initial pHs (A), initial tryptone concentrations (B), and initial DC concentrations (C).

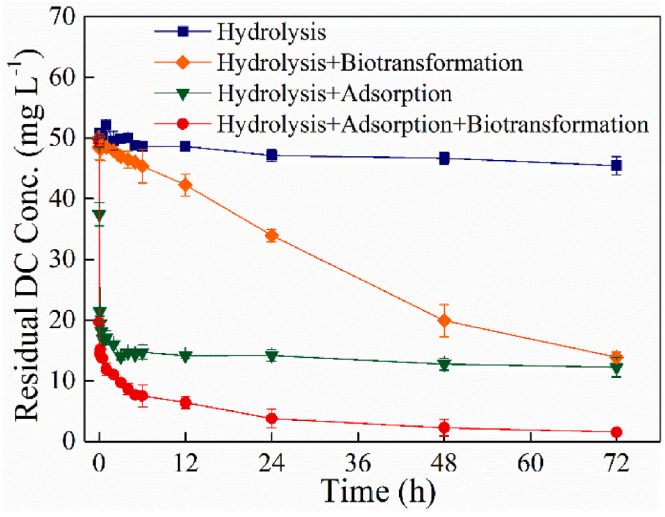

Fig. 4. DC was removed by hydrolysis (solution only), hydrolysis + biotransformation (DD1), hydrolysis + adsorption (RSPs), hydrolysis + adsorption + biotransformation (DD1-RSPs) at T = 20 °C, pH = 7, tryptone = 4 g L^{-1}, and initial DC = 50 mg L^{-1}. Error bars were standard deviations from triplicate experiments.

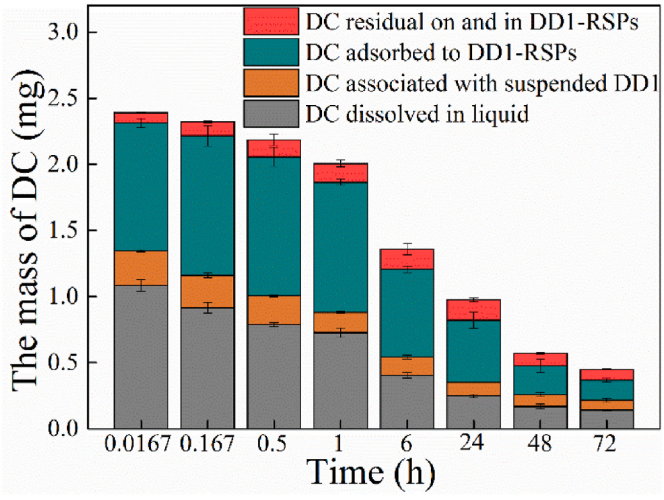

Fig. 5. The DC distribution in four positions of the solution containing DD1-RSPs. Error bars were standard deviations from triplicate experiments. The procedure to measure DC in each compartment is presented in Fig. 1.

was converted to DP-428 by losing the amino group of the amide group at C2. DP-428 was further converted to DP 410 by having the hydroxyl at C5 removed or converted to DP-400 by having the carbonyl group at C1 removed. In the third pathway, the oxidation of DC at the C8–C9 resulted in the formation of DP-461. DP-461 lost the hydroxyl group at

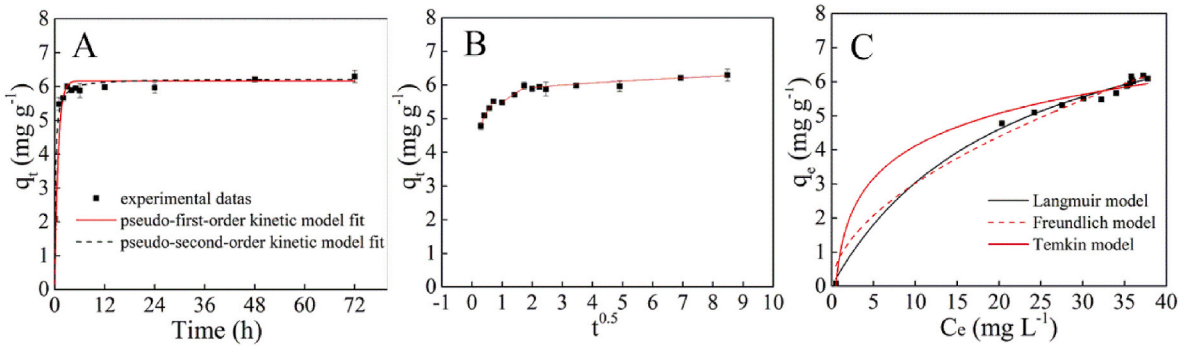

Fig. 6. The pseudo-first-order and pseudo-second-order kinetic models of DC adsorption on RSPs (A), the intra-particle diffusion kinetics (B), three different isotherm kinetic models of DC adsorption on RSPs (C).

Table 2
Characteristics of the parent compound and the products from hydrolysis, adsorption and/or biotransformation of DC.

Time (min)	Name	Compound Ion	Predicted Mass (*m/z*)	Measured mass (*m/z*)	Error (ppm)	Elemental composition	Ring Double bond equivalent value (RDB)	Intensity	MS-MS
5.88		ISO-DC or EDC $[M+H]^+$	445.1605	445.1608	0.67	$C_{22}H_{25}O_8N_2$	11.5	2.56e+008	428, 410
6.54	DC	DC-445 $[M+H]^+$	445.1605	445.1612	1.57	$C_{22}H_{25}O_8N_2$	11.5	1.89e+008	428, 410
3.91	DP-461	$[M + H + O]^+$	461.1555	461.1556	0.22	$C_{22}H_{25}O_9N_2$	11.5	1.02e+006	388
3.80	DP-459	$[M + H + O–2H]^+$	459.1398	459.1392	1.30	$C_{22}H_{23}O_9N_2$	12.5	1.28e+004	395
5.84	DP-443	$[M + H + O–H_2O]^+$	443.1449	443.1442	1.57	$C_{22}H_{23}O_8N_2$	12.5	3.43 + 005	426
6.73	DP-428	$[M + H–NH_3]^+$ or $[M + H + O–H_2O–NH]^+$	428.1340	428.1326	3.27	$C_{22}H_{22}O_8N$	12.5	1.24e+007	410,392
4.02	DP-417	$[M + H–CO]^+$	417.1656	417.1652	0.96	$C_{21}H_{25}O_7N_2$	10.5	1.26e+007	400, 382
6.34	DP-410	$[M + H–NH_3–H_2O]^+$ or $[M + H + O–H_2O–NH–H_2O]^+$	410.1234	410.1237	0.73	$C_{22}H_{20}O_7N$	13.5	2.38e+005	367, 339
5.70	DP-402	$[M + H–CO–NH]^+$	402.1547	402.1542	1.24	$C_{21}H_{24}O_7N$	10.5	1.19e+006	384, 366
4.07	DP-400	$[M + H–NH_3–CO]^+$ or $[M + H + O–H_2O–NH–CO]^+$	400.1391	400.1383	2.00	$C_{21}H_{22}O_7N$	11.5	3.22e+005	382
7.62	DP-338	$[M + H–CO–NH–CO–2H_2O]^+$	338.1387	338.1391	1.18	$C_{20}H_{20}O_4N$	11.5	6.47e+004	–
8.03	DP-323	$[M + H–CO–NH–CO–2H_2O–CH_2–OH + NH_2]^+$	323.1390	323.1389	0.31	$C_{19}H_{19}O_3N_2$	11.5	1.84e+005	323, 277

C5 to form DP-443. Subsequently, DP-443 lost the amino group of the amide group at C2 and was converted to DP-428. Further, the hydroxyl at C12a was removed to form DP-410, or the carbonyl group at C1 or C2 was removed to form DP-400.

4. Discussion

4.1. Effects of pH & tryptone on the hydrolysis, adsorption and biotransformation of DC

Hydrolysis and adsorption of DC increased with the increase of pH. DC is an amphiphilic molecule with three acid dissociation constants (pK_a = 3.50, 7.07, 9.13) and multiple ionizable functional groups (Bolobajev et al., 2016). When the pH of the solution increased from 6 to 10, DC mainly existed in the form of zwitterions. Species with different degrees of ionization dominated the solution at different pHs, resulting in different hydrolysis rates (Chao et al., 2014; Liu et al., 2019). The acidic condition is conducive to the stability of DC, while the alkaline condition has the opposite effects (Pouliquen et al., 2007; Fu et al., 2017). In addition, the main functional group of native RSPs is the hydroxyl group (Gong et al., 2006). Because DC competed with hydrogen ions, which decreased in solution as pH increased, for adsorption sites on RSPs, DC adsorption faced less competition and therefore gradually increased as pH increased (Gong et al., 2006). In contrast, DC biotransformation decreased as pH increased (Fig. 3A–iii), which may be due to the inhibition of bacterial growth and enzyme activities at higher pHs (Wu et al., 2019).

DD1 couldn't use DC as a sole energy source to grow (Fig. S3). As the primary substrate, tryptone provided carbon and nitrogen sources to DD1 and promoted DC biotransformation. During co-metabolisms, catabolic enzymes for non-growth substrate are produced in the process of primary growth substrate. Hence, growth substrate concentrations often affect the co-metabolism of non-growth substrate (Luo et al., 2008). Unlike for biotransformation, tryptone had a negative effect on the adsorption of DC onto RSPs (Fig. 3B–ii), as organic compounds likes tryptone could compete with DC for adsorption sites on RSPs (Zhang and He, 2013).

4.2. Kinetics and mechanisms of DC adsorption to RSPs

The pseudo-second-order model could better describe the kinetics of DC adsorption to RSPs than the pseudo-first-order model. This finding is consistent with previous findings that the pseudo-second-order model could describe the adsorption kinetics of TCs to various adsorbents

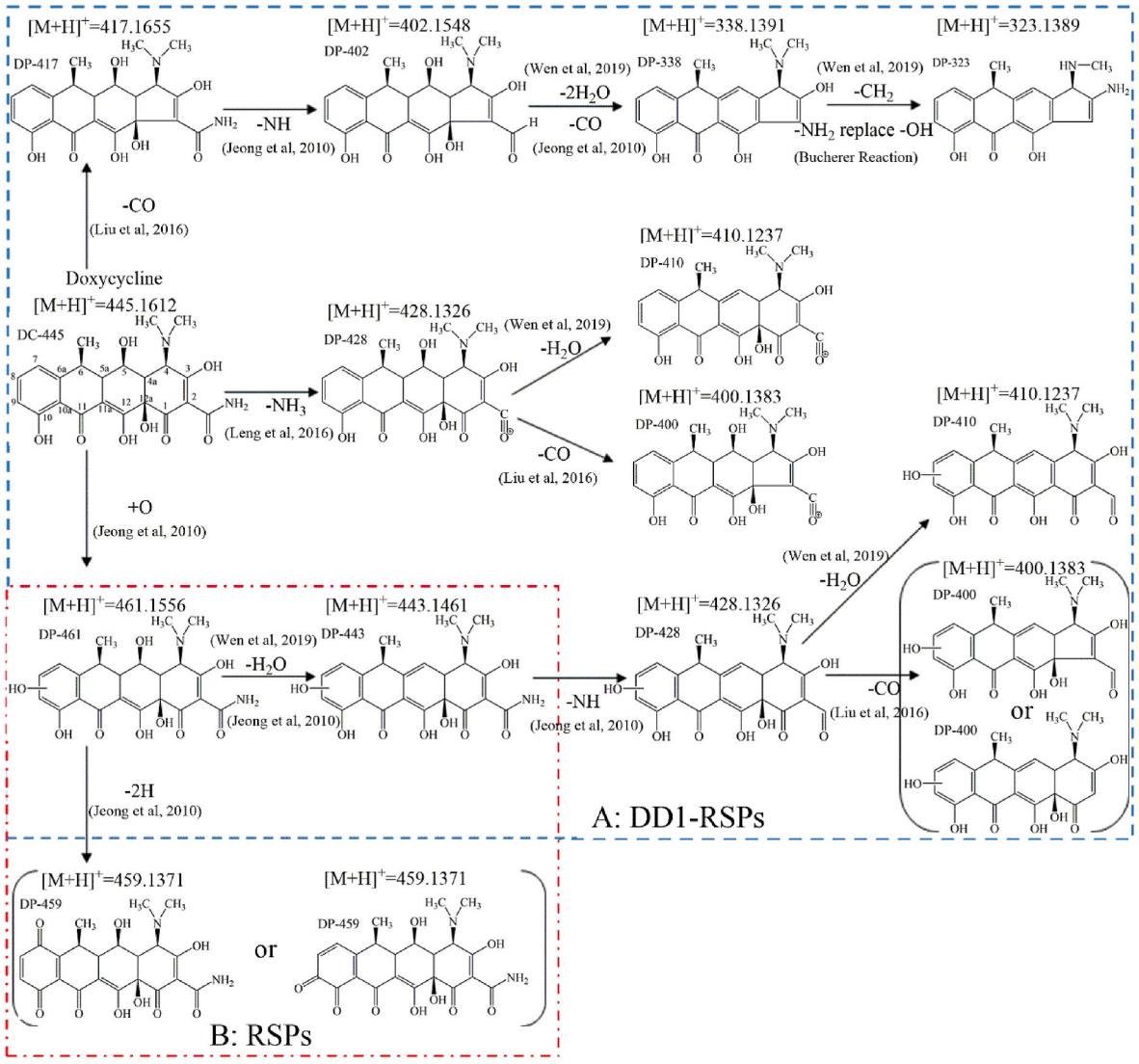

Fig. 7. Degradation pathways of DC in solution containing DD1-RSPs (A) and RSPs (B).

(Priya and Radha, 2017). The kinetic model suggests that DC was mainly adsorbed onto the surface of RSPs by chemical interactions, such as hydrogen bonding (Zeng et al., 2018b). Intraparticle diffusion kinetics suggested that initially DC quickly adsorbed on the exterior of DD1-RSPs and then the adsorption slowed down during the intraparticle diffusion due to lower DC concentration, smaller pores and fewer adsorption sites (Hameed et al., 2008). Moreover, because the curves of three stages didn't cross the origin (Fig. 6B), the intraparticle diffusion might not be the only rate control step in the adsorption process (Hameed et al., 2008; Liu et al., 2017; Wei et al., 2019). The fitting of the isotherm data with the Langmuir model (Fig. 6C) suggests DC adsorbed on RSPs through chemisorption (Priya and Radha, 2017) and formed a monolayer (Liu et al., 2017). The K_L of our study was 0.0469 ± 0.0070 L mg^{-1}, suggesting that the adsorption between DC and RSPs was favorable (Tan et al., 2016).

4.3. Synergistic removal of DC by adsorption and biotransformation

DC was adsorbed rapidly, because RSPs contained high surface areas (e.g., 1.229 m^2/g (Wang et al., 2016) and 1.533 m^2/g (Wi et al., 2013)) and porous structure (Fig. 1), allowing for DC adsorption both on the surface and the interior of the pores (Rocha et al., 2009). Based on the results presented in Figs. 4–6, we propose the following process where adsorption and biotransformation worked synergistically to remove DC from water (Kannan and Sundaram, 2001; Gong et al., 2006). The first-order reaction rate constants for abiotic processes such as UV treatment and advanced oxidation processes were reported to range between 0.14×10^{-1} to 3.1×10^{-1} min^{-1} (Bolobajev et al., 2016). In comparison, the first-order reaction rate constant for the adsorption process in this study is about 2.9×10^{-1} min^{-1}. The kinetic of the combined adsorption and biotransformation process was noticeably faster than the adsorption process along (Fig. 4), as bacteria could degrade adsorbed DC to free up more adsorption sites on RSP surface. Moreover, compared to free cells, solid surface often provides a more stable living environment for microorganisms (Xue et al., 2019). As illustrated in the Graphic Abstract, dissolved DC in the solution first adsorbed to the boundary layer of RSPs and diffused through the boundary layer to reach the surface of RSPs. Second, DC adsorbed on the active sites on the exterior and the pore of RSPs. Third, DC reached the deeper portion of the pores of RSPs through intraparticle diffusion. Fourth, DC was biotransformed by the DD1 cells on and in the DD1-RSP matrix. Overall, the combined mechanisms of adsorption and biodegradation synergistically and efficiently removed DC from water.

4.4. Transformation products

TC antibiotics share similar transformation products and pathways due to the similarities in their molecular structures. Between pH 6 and 10, hydrolysis can cause conversion of DC to its isomer or epimer without forming other transformation products. Biotransformation products were formed in the presence of DD1. The transformation pathway that involved DP-417, DP-402, DP-338, DP-323 has been reported in our previous study (He et al., 2021). The other two pathways, which included conversion of DC to DP-428 and to DP-461, respectively, are reported for the first time. In the pathway that involves DP-461, the oxidation of C═C double bond between C8 and C9 resulted in DP-461 (Jeong et al., 2010). The sequential loss of the hydroxyl group on C5 and C12a was reported in a reaction where photocatalyst Ag/AgCl–CdMoO4 was used to treat DC (Wen et al., 2019).

In the pathway that involves DP-428, $–NH_3$ at C2 was lost to form DP-428. This process was also reported in the biotransformation of tetracycline by *S. maltophilia* (Leng et al., 2016), by the catalysis of laccase (De Cazes et al., 2014), and by mixed microbial community (Cai et al., 2018). Similar to the degradation of oxytetracyline, the decarbonylation reaction at C1 is similar to the degradation of oxytetracycline (Liu et al., 2016). During the process, an α-cleavage occurred at the C1–C12a bond, forming a diradical intermediate. The resulting diradical intermediate then lost a carbonyl group and formed another diradical, which closed the ring (i.e., DP-428 to DP-400).

5. Conclusions

In this study, rice straw particles and *B. naejangsanensis* DD1 were mixed to make a cell-covered adsorbent, DD1-RSPs. Under the optimal condition determined for individual processes, the removal of DC by adsorption and biodegradation was characterized. Compared to the slower kinetics of biotransformation by DD1 alone, DD1-RSPs could quickly remove DC from water by adsorption within a few hours. Compared to lower removal of DC by adsorption to RSPs alone, DD1-RSPs could remove more DC from water. In addition, the adsorption of DC to RSPs can be explained using the pseudo-second-order kinetics and the Langmuir isotherm. Through a series of demethylation, dehydration, and deamination, decarbonylation, DC was converted by the DD1 cells on DD1-RSPs to biotransformation products DP-410, DP-400, and DP-323. The findings of this study demonstrate the feasibility and advantages of using DD1-RSPs to remove DC from water.

Credit author statement

Ting He: Data curation, Formal analysis, Investigation, Methodology, Writing-original draft. Jianguo Bao: Conceptualization, Funding acquisition, Methodology, Supervision, Writing – review and editing. Yifei Leng: Data curation, Methodology, Writing – original draft. Shuqiong Kong: Investigation, Methodology. Jiangkun Du: Investigation, Methodology. Xu Li: Conceptualization, Funding acquisition, Methodology, Supervision, Writing – review and editing.

Declaration of competing interest

The authors declare that they have no known competing financial interests or personal relationships that could have appeared to influence the work reported in this paper.

Acknowledgements

The authors would like to thank the financial support from the National Natural Science Foundation of China (41373083 and 42077312), National Key R&D Program – International S&T Development (2021YFE0106600), and the National Science Foundation (1351676 and 1805990).

Appendix A. Supplementary data

Supplementary data to this article can be found online at https://doi.org/10.1016/j.chemosphere.2021.132828.

References

Abbas, R.F., Hami, H.K., Mahdi, N.I., 2018. Removal of doxycycline hyclate by adsorption onto cobalt oxide at three different temperatures: isotherm, thermodynamic and error analysis. Int. J. Environ. Sci. Technol. 16, 5439–5446.
Adamek, E., Baran, W., Sobczak, A., 2016. Photocatalytic degradation of veterinary antibiotics: biodegradability and antimicrobial activity of intermediates. Process Saf. Environ. Protect. 103, 1–9.
Ahmed, M.J., 2016. Preparation of activated carbons from date (*Phoenix dactylifera* L.) palm stones and application for wastewater treatments: Review. Process Saf. Environ. Protect. 102, 168–182.
Bai, B., Xu, X., Li, C., Xing, J., Wang, H., Suo, Y., 2018. Magnetic Fe_3O_4@chitosan carbon microbeads: removal of doxycycline from aqueous solutions through a fixed bed via sequential adsorption and heterogeneous Fenton-like regeneration. J. Nanomater. 1–14, 2018.
Bolobajev, J., Trapido, M., Goi, A., 2016. Effect of iron ion on doxycycline photocatalytic and Fenton-based autocatatalytic decomposition. Chemosphere 153, 220–226.
Brigante, M., Avena, M., 2016. Biotemplated synthesis of mesoporous silica for doxycycline removal. Effect of pH, temperature, ionic strength and Ca^{2+} concentration on the adsorption behaviour. Microporous Mesoporous Mater. 225, 534–542.
Cai, M., Ma, S., Hu, R., Tomberlin, J.K., Yu, C., Huang, Y., Zhan, S., Li, W., Zheng, L., Yu, Z., Zhang, J., 2018. Systematic characterization and proposed pathway of tetracycline degradation in solid waste treatment by *Hermetia illucens* with intestinal microbiota. Environ. Pollut. 242, 634–642.
Chao, Y., Zhu, W., Wu, X., Hou, F., Xun, S., Wu, P., Ji, H., Xu, H., Li, H., 2014. Application of graphene-like layered molybdenum disulfide and its excellent adsorption behavior for doxycycline antibiotic. Chem. Eng. J. 243, 60–67.
Chen, H., Chen, X., Qin, Y., Wei, J., Liu, H., 2017. Effect of torrefaction on the properties of rice straw high temperature pyrolysis char: pore structure, aromaticity and gasification activity. Bioresour. Technol. 228, 241–249.
Dada, A.O., Olalekan, A.P., Olatunya, A.M., Dada, O., 2012. Langmuir, Freundlich, Temkin and Dubinin–Radushkevich isotherms studies of equilibrium sorption of Zn^{2+} unto phosphoric acid modified rice husk. IOSR J. Appl. Chem. 3, 38–45.
Dai, Y., Sun, Q., Wang, W., Lu, L., Liu, M., Li, J., Yang, S., Sun, Y., Zhang, K., Xu, J., Zheng, W., Hu, Z., Yang, Y., Gao, Y., Chen, Y., Zhang, X., Gao, F., Zhang, Y., 2018. Utilizations of agricultural waste as adsorbent for the removal of contaminants: a review. Chemosphere 211, 235–253.
De Cazes, M., Belleville, M.P., Petit, E., Llorca, M., Rodríguez-Mozaz, S., de Gunzburg, J., Barceló, D., Sanchez-Marcano, J., 2014. Design and optimization of an enzymatic membrane reactor for tetracycline degradation. Catal. Today 236, 146–152.
Deng, W., Li, N., Zheng, H., Lin, H., 2016. Occurrence and risk assessment of antibiotics in river water in Hong Kong. Ecotoxicol. Environ. Saf. 125, 121–127.
Dzionek, A., Wojcieszyńska, D., Guzik, U., 2016. Natural carriers in bioremediation: a review. Electron. J. Biotechnol. 23, 28–36.
Fan, Y., Zheng, C., Hou, H., 2019. Preparation of granular activated carbon and its mechanism in the removal of isoniazid,sulfamethoxazole,thiamphenicol,and doxycycline from aqueous solution. Environ. Eng. Sci. 36, 1027–1040.
Fu, L., Huang, T., Wang, S., Wang, X., Su, L., Li, C., Zhao, Y., 2017. Toxicity of 13 different antibiotics towards freshwater green algae *Pseudokirchneriella subcapitata* and their modes of action. Chemosphere 168, 217–222.
Fuentes, M.D., Gutierrez, S., Sahagun, D., Gomez, J., Mendoza, J., Ellis, C.C., Bauer, S., Blattner, J., Lee, Y.W., Alvarez, M., Domínguez, D.C., 2019. Assessment of antibiotic levels, multi-drug resistant bacteria and genetic biomarkers in the waters of the rio grande river between the United States-Mexico border. J. Health Pollut. 9, 1–13.
Gong, R., Jin, Y., Chen, F., Chen, J., Liu, Z., 2006. Enhanced malachite green removal from aqueous solution by citric acid modified rice straw. J. Hazard Mater. 137, 865–870.
Gopal, G., Alex, S.A., Chandrasekaran, N., Mukherjee, A., 2020. A review on tetracycline removal from aqueous systems by advanced treatment techniques. RSC Adv. 10, 27081–27095.
Hameed, B.H., Tan, I.A.W., Ahmad, A.L., 2008. Adsorption isotherm, kinetic modeling and mechanism of 2,4,6-trichlorophenol on coconut husk-based activated carbon. Chem. Eng. J. 144, 235–244.
Heaton, P.C., Fenwick, S.R., Brewer, D.E., 2007. Association between tetracycline or doxycycline and hepatotoxicity-a population based case-control study 1. J. Clin. Pharm. Therapeut. 32, 483–487.
He, T., Bao, J., Leng, Y., Snow, D., Kong, S., Wang, T., Li, X., 2021. Biotransformation of doxycycline by *Brevundimonas naejangsanensis* and *Sphingobacterium mizutaii* strains. J. Hazard Mater. 411, 125126.
Ho, Y.B., Zakaria, M.P., Latif, P.A., Saari, N., 2014. Occurrence of veterinary antibiotics and progesterone in broiler manure and agricultural soil in Malaysia. Sci. Total Environ. 488–489, 261–267.
Jeong, J., Song, W., Cooper, W.J., Jung, J., Greaves, J., 2010. Degradation of tetracycline antibiotics: mechanisms and kinetic studies for advanced oxidation/reduction processes. Chemosphere 78, 533–540.
Karimi, K., Kheradmandinia, S., Taherzadeh, M.J., 2006. Conversion of rice straw to sugars by dilute-acid hydrolysis. Biomass Bioenergy 30, 247–253.

Kannan, N., Sundaram, M.M., 2001. Kinetics and mechanism of removal of methylene blue by adsorption on various carbons—a comparative study. Dyes Pigments 51, 25–40.
Leng, Y., Bao, J., Chang, G., Zheng, H., Li, X., Du, J., Snow, D., Li, X., 2016. Biotransformation of tetracycline by a novel bacterial strain *Stenotrophomonas maltophilia* DT1. J. Hazard Mater. 318, 125–133.
Liao, Q., Rong, H., Zhao, M., Luo, H., Chu, Z., Wang, R., 2021. Interaction between tetracycline and microorganisms during wastewater treatment: a review. Sci. Total Environ. 757, 143981.
Lin, J., Gan, L., Chen, Z., Naidu, R., 2015. Biodegradation of tetradecane using *Acinetobacter venetianus* immobilized on bagasse. Biochem. Eng. J. 100, 76–82.
Lindberg, R.H., Wennberg, P., Johansson, M.I., Tysklind, M., Andersson, B.A.V., 2005. Screening of human antibiotic substances and determination of weekly mass flows in five sewage treatment plants in Sweden. Environ. Sci. Technol. 39, 3421–3429.
Liu, S., Xu, W.H., Liu, Y.G., Tan, X.F., Zeng, G.M., Li, X., Liang, J., Zhou, Z., Yan, Z.L., Cai, X.X., 2017. Facile synthesis of Cu(II) impregnated biochar with enhanced adsorption activity for the removal of doxycycline hydrochloride from water. Sci. Total Environ. 592, 546–553.
Liu, S.J., Liu, Y.G., Tan, X.F., Liu, S.B., Li, M.F., Liu, N., Yin, Z.H., Tian, S.R., Zhou, Y.H., 2019. Facile synthesis of MnOx-loaded biochar for the removal of doxycycline hydrochloride: effects of ambient conditions and co-existing heavy metals. J. Chem. Technol. Biotechnol. 94, 2187–2197.
Liu, W., Zhou, J., Zhou, J., 2018. Facile fabrication of multi-walled carbon nanotubes (MWCNTs)/α-Bi_2O_3 nanosheets composite with enhanced photocatalytic activity for doxycycline degradation under visible light irradiation. J. Mater. Sci. 54, 3294–3308.
Liu, Y., He, X., Fu, Y., Dionysiou, D.D., 2016. Degradation kinetics and mechanism of oxytetracycline by hydroxyl radical-based advanced oxidation processes. Chem. Eng. J. 284, 1317–1327.
Luo, W., Zhao, Y., Ding, H., Lin, X., Zheng, H., 2008. Co-metabolic degradation of bensulfuron-methyl in laboratory conditions. J. Hazard Mater. 158, 208–214.
Ma, Y., Li, M., Wu, M., Li, Z., Liu, X., 2015. Occurrences and regional distributions of 20 antibiotics in water bodies during groundwater recharge. Sci. Total Environ. 518–519, 498–506.
Olusegun, S.J., Mohallem, N.D.S., 2019. Insight into the adsorption of doxycycline hydrochloride on different thermally treated hierarchical $CoFe_2O_4$/bio-silica nanocomposite. J. Environ. Chem. Eng. 7, 103442.
Pouliquen, H., Delépée, R., Larhantec-Verdier, M., Morvan, M.L., Le Bris, H., 2007. Comparative hydrolysis and photolysis of four antibacterial agents (oxytetracycline oxolinic acid, flumequine and florfenicol) in deionised water, freshwater and seawater under abiotic conditions. Aquaculture 262, 23–28.
Priya, S.S., Radha, K.V., 2017. A review on the adsorption studies of tetracycline onto various types of adsorbents. Chem. Eng. Commun. 204, 821–839.
Rocha, C.G., Zaia, D.A., Alfaya, R.V., Alfaya, A.A., 2009. Use of rice straw as biosorbent for removal of Cu(II), Zn(II), Cd(II) and Hg(II) ions in industrial effluents. J. Hazard Mater. 166, 383–388.
Ruan, B., Wu, P., Chen, M., Lai, X., Chen, L., Yu, L., Gong, B., Kang, C., Dang, Z., Shi, Z., Liu, Z., 2018. Immobilization of *Sphingomonas sp.* GY2B in polyvinyl alcohol-alginate-kaolin beads for efficient degradation of phenol against unfavorable environmental factors. Ecotoxicol. Environ. Saf. 162, 103–111.
Shao, S., Wu, X., 2020. Microbial degradation of tetracycline in the aquatic environment: a review. Crit. Rev. Biotechnol. 40, 1010–1018.
Song, C., Sun, X.F., Wang, Y.K., Xia, P.F., Yuan, F.H., Li, J.J., Wang, S.G., 2016. Fate of tetracycline at high concentrations in enriched mixed culture system: biodegradation and behavior. J. Chem. Technol. Biotechnol. 91, 1562–1568.
Spina-Cruz, M., Maniero, M.G., Guimaraes, J.R., 2019. Advanced oxidation processes on doxycycline degradation: monitoring of antimicrobial activity and toxicity. Environ. Sci. Pollut. Res. Int. 26, 27604–27619.
Tan, X., Liu, S., Liu, Y., Gu, Y., Zeng, G., Cai, X., Yan, Z., Yang, C., Hu, X., Chen, B., 2016. One-pot synthesis of carbon supported calcined-Mg/Al layered double hydroxides for antibiotic removal by slow pyrolysis of biomass waste. Sci. Rep. 6, 39691.
Tong, Y., Kang, J., Shen, J., Chen, Z., Zhao, S., Sun, L., Wang, W., 2019. Effective degradation of doxycycline by photocatalytic $BiVO_4$–H_2O_2 under visible light. Environ. Progress Sustain 38.
Wang, J.Y., Cui, H., Cui, C.W., Xing, D.F., 2016. Biosorption of copper(II) from aqueous solutions by Aspergillus Niger-treated rice straw. Ecol. Eng. 95, 793–799.
Wang, W., Han, Q., Zhu, Z., Zhang, L., Zhong, S., Liu, B., 2019. Enhanced photocatalytic degradation performance of organic contaminants by heterojunction photocatalyst $BiVO_4$/TiO_2/RGO and its compatibility on four different tetracycline antibiotics. Adv. Powder Technol. 30, 1882–1896.
Wei, J., Liu, Y., Li, J., Zhu, Y., Yu, H., Peng, Y., 2019. Adsorption and co-adsorption of tetracycline and doxycycline by one-step synthesized iron loaded sludge biochar. Chemosphere 236, 124254.
Wen, X., Shen, C., Niu, C., Lai, D., Zhu, M., Sun, J., Hu, Y., Fei, Z., 2019. Attachment of Ag/AgCl nanoparticles on $CdMoO_4$ microspheres for effective degradation of doxycycline under visible light irradiation: degradation pathways and mineralization activity. J. Mol. Liq. 288, 111063.
Wen, X., Wang, Y., Zou, Y., Ma, B., Wu, Y., 2018. No evidential correlation between veterinary antibiotic degradation ability and resistance genes in microorganisms during the biodegradation of doxycycline. Ecotoxicol. Environ. Saf. 147, 759–766.
Wi, S.G., Choi, I.S., Kim, K.H., Kim, H.M., Bae, H.J., 2013. Bioethanol production from rice straw by popping pretreatment. Biotechnol. Biofuels 6, 166.
Widyasari-Mehta, A., Suwito, H.R., Kreuzig, R., 2016. Laboratory testing on the removal of the veterinary antibiotic doxycycline during long-term liquid pig manure and digestate storage. Chemosphere 149, 154–160.
Wu, X., Wu, X., Shen, L., Li, J., Yu, R., Liu, Y., Qiu, G., Zeng, W., 2019. Whole genome sequencing and comparative genomics analyses of *Pandoraea sp.* XY-2, a new species capable of biodegrade tetracycline. Front. Microbiol. 10, 33.
Wu, X., Zhou, X., Wu, X., Gu, Y., Zhou, H., Shen, L., Zeng, W., 2020. Optimization of whole-cell immobilization system constructed with two-species microorganism and its ability of tetracycline wastewater treatment. Int. J. Environ. Sci. Technol. 18, 471–482.
Xie, B., Tang, X., Ng, H.Y., Deng, S., Shi, X., Song, W., Huang, S., Li, G., Liang, H., 2020. Biological sulfamethoxazole degradation along with anaerobically digested centrate treatment by immobilized microalgal-bacterial consortium: performance, mechanism and shifts in bacterial and microalgal communities. Chem. Eng. J. 388, 124217.
Xu, L., Zhang, H., Xiong, P., Zhu, Q., Liao, C., Jiang, G., 2021. Occurrence, fate, and risk assessment of typical tetracycline antibiotics in the aquatic environment: a review. Sci. Total Environ. 753, 141975.
Xue, J., Wu, Y., Shi, K., Xiao, X., Gao, Y., Li, L., Qiao, Y., 2019. Study on the degradation performance and kinetics of immobilized cells in straw-alginate beads in marine environment. Bioresour. Technol. 280, 88–94.
Yan, Q., Li, X., Ma, B., Zou, Y., Wang, Y., Liao, X., Liang, J., Mi, J., Wu, Y., 2018. Different concentrations of doxycycline in swine manure affect the microbiome and degradation of doxycycline residue in soil. Front. Microbiol. 9, 3129.
Zaidi, S., Sivasankar, V., Chaabane, T., Alonzo, V., Omine, K., Maachi, R., Darchen, A., Prabhakaran, M., 2019. Separate and simultaneous removal of doxycycline and oxytetracycline antibiotics by electro-generated adsorbents (EGAs). J. Environ. Chem. Eng. 7, 102876.
Zaranyika, M.F., Dzomba, P., Kugara, J., 2015. Speciation and persistence of doxycycline in the aquatic environment: characterization in terms of steady state kinetics. J. Environ. Sci. Health. B 50, 908–918.
Zeng, Z.W., Tian, S.R., Liu, Y.G., Tan, X.Y., Zeng, G.M., Jiang, L.H., Yin, Z.H., Liu, N., Liu, S.B., Li, J., 2018a. Comparative study of rice husk biochars for aqueous antibiotics removal. J. Chem. Technol. Biotechnol. 93, 1075–1084.
Zeng, Z.W., Tan, X.F., Liu, Y.G., Tian, S.R., Zeng, G.M., Jiang, L.H., Liu, S.B., Li, J., Liu, N., Yin, Z.H., 2018b. Comprehensive adsorption studies of doxycycline and ciprofloxacin antibiotics by biochars prepared at different temperatures. Front. Chem. 6, 80.
Zhang, J., He, M., 2013. Effect of dissolved organic matter on sorption and desorption of phenanthrene onto black carbon. J. Environ. Sci. 25, 2378–2383.
Zhang, W., Ren, X., He, J., Zhang, Q., Qiu, C., Fan, B., 2019. Application of natural mixed bacteria immobilized carriers to different kinds of organic wastewater treatment and microbial community comparison. J. Hazard Mater. 377, 113–123.
Zhang, X., Bai, B., Li Puma, G., Wang, H., Suo, Y., 2016a. Novel sea buckthorn biocarbon SBC@β-FeOOH composites: efficient removal of doxycycline in aqueous solution in a fixed-bed through synergistic adsorption and heterogeneous Fenton-like reaction. Chem. Eng. J. 284, 698–707.
Zhang, X., Bai, B., Wang, H., Suo, Y., 2016b. Facile fabrication of sea buckthorn biocarbon (SB)@α-Fe_2O_3 composite catalysts and their applications for adsorptive removal of doxycycline wastewater through a cohesive heterogeneous Fenton-like regeneration. RSC Adv. 6, 38159–38168.